LIGO-T960002-00-R

MOSCOW STATE UNIVERSITY

Department of Physics

# SUSPENSIONS AND SUSPENSION NOISE FOR *LIGO* TEST MASSES

Annual report 1995 (Grant No. PHY-9503642)

The contributors:

A.J. Ageev
I.A Bilenko
V.B. Braginsky (PI)
V.S. Ilchenko
A.A. Khorev
V.P. Mitrofanov
K.V. Tokmakov
S.P. Vyatchanin

The content :

## 1. Measurement of the quality factor of the torsional-pendulum mode of two-fibers suspension fused silica pendulum.

We tested quality factor of the low frequency mode of oscillations for fused silica cylinder (10 cm D, 12 cm L) with intermediate mass about M ≈ 2 kg, suspended on two fused silica fibers (2r ≈ 150-200 μm, L ≈ 20 cm). Fibers were welded to two ridges, carved in the middle of the cylinder.

The key problem to realize the measurement $Q^{-1}$ of pendulum mode for a heavy mass pendulum is the reduction of the recoil losses in the support.

In order to overcome this obstacle it is reasonable not to measure the losses in the ordinary pendulum but instead, to measure the Q of the torsional mode of the cylinder suspended on two fibers. In this case, the fibers are bending in the process of torsional oscillation similar to that in an ordinary pendulum, and thus Q must be close to $Q_{pendul}$. Fig.1 presents the design of the pendulum suspended inside a rigid "cage" made of aluminum alloy.

In addition in this design it is easier to provide more rigid support for torsional motion than for bending motion.

In case of combine torsional-pendulum mode the predicted Q limited by the fiber material losses ( $\Phi_G \approx \Phi_Y \approx Q^{-1}_{silica} \approx 1.4 \cdot 10^{-7}$ ) is defined by the following formula:

$$Q^{-1} \approx \frac{\pi G r^4}{Mga^2} \Phi_G + \frac{\sqrt{TYJ}}{2MgL} \Phi_Y ,$$

where G and Y are shear and Young module of the fiber material,

(2a) - a distance between the fibers, J - a momentum of inertia of the fiber cross section, T = Mg/2 - a tension in fibers.

For the tested pendulums this predicted value $Q^{-1} \approx 3 \cdot 10^{-9}$.

Fig. 2 and 3 present the measured time dependence of amplitude of torsional-pendulum mode free oscillations for two double fiber pendulums. The frequency of this mode is $f_0 \approx 0.34$ Hz in both cases. For the first pendulum, the value of the relaxation time $\tau^*$, evaluated from the plot, is equal to $4.8 \cdot 10^7$s ( $Q_{t-p} = 5.3 \cdot 10^7$); for the second one $\tau^* = 4.6 \cdot 10^7$s ($Q_{t-p} = 4.9 \cdot 10^7$).

The first pendulum was tested at the pressure $p = 2 \cdot 10^{-6}$Torr, the second one - at $p = 1 \cdot 10^{-6}$ Torr. For such pressures it is necessary to make the correction caused by a residual gas damping. With this correction (its contribution was obtained by extrapolation of measured pressure-damping dependence for these pendulums into the region of low pressure) the quality factors are $Q_1 = 1 \cdot 10^8 (\pm 25\%)$ and $Q_2 = 6.5 \cdot 10^7 (\pm 15\%)$.

The obtained values of Q are substantially higher than any values of pendulum modes obtained by other research groups. At the same time, the obtained values $Q_{t-p}$, as well as the $Q_{violin}$ ( see the report of MSU group, 1994 ) are smaller, than theoretical expectation. On our opinion, the discrepancy for $Q_{t-p}$ can be explained by the leak of the energy into support. This discrepancy motivates us to continue the search for the ultimate value of $Q_{pendul}$.

## 2. Experimental system for excess noise measurement in suspension wires: design and tests.

We have designed experimental setup to meet specific requirements of the long term excess noise measurement. At the first step of the project we decided to investigate the behavior of a 15 cm-long tungsten wires with diameters ranged from 0.02 to 0.1 mm. Such a wire should be a good model of the suspension wires in the gravitational antenna mirror. To detect whether the excess noise really exists, one should monitor thermal motion of the center of the loaded wire. If one takes into account only fundamental violin mode of the oscillations, the amplitude of the Brownian motion for the wire is

$$\sqrt{\langle \Delta x^2 \rangle} = \frac{1}{\omega d}\sqrt{\frac{8kT}{\pi \rho l}},$$

here $\omega$ is the eigenfrequency of the fundamental violin mode, d - wire diameter, l - its length, $\rho$ is the material volume density, k - Boltzman constant, T - temperature. With d = 0.02 mm, l=15 cm the value of $\omega$ is of the order $1.5 \cdot 10^4$ $sec^{-1}$ for the tungsten wire and the magnitude of the thermal oscillation is of order $9 \times 10^{-10}$ cm.

To make a conclusion about the statistics of the noise process one can estimate the rate of the peaks, exceeding some given threshold. The readout device has to be sensitive enough to displacement within rather wide bandwidth.

In addition, it is important to avoid any external influence on the wire under study. It is not reasonable to attach anything

to the wire directly because noise properties depend on surface conditions.

Laser interferometric method has been chosen to satisfy the above condition. The Michelson-like interferometer has been designed and tested. Wire samples mounted on a rigid frame and readout interferometer are placed in the vacuum chamber. The pressure in the chamber is about $1\times10^{-3}$ Torr, which is sufficient to avoid viscous gas damping of the wire oscillation. The turbomolecular pump is used for the preliminary evacuation, and the absorption cryopump allows to keep low pressure during the experiment without undesirable mechanical vibration.

The helium-neon stabilized laser is used as a pump source. The standard 0.9 mW single mode laser has been equipped with additional system of the active amplitude stabilization. The system consists of the photodetector placed inside the vacuum chamber, low noise amplifier, RF filter and electro-optical modulator. The application of this system allows to improve the pump source noise performance decreasing the spectral density of relative fluctuations of power from $3\times10^{-5}$ $Hz^{-1/2}$ to $5\times10^{-6}$ $Hz^{-1/2}$.

The schematic of the interferometer is given on Fig.4. The interferometer consists of beam splitter (1), fixed mirror (2), lens system (3), reference arm mirror (4) and object surface (5). Two beams, formed by splitter and fixed mirror, pass through the lenses system and one beam is focused on the wire surface and the other one - on reference mirror. To separate those two focal points one has to provide small angle between the beams. In our case this angle is of order $15^{\circ}$, and the distance between the

focal points is 1.5 mm. The reflected light passing back to beam splitter is recombined further on the detector. The diaphragm is used to select zero order fringe. The lens system allows us to prepare focal spot of 5 μm in diameter sufficient for the 20 μm wire. In this type of interferometer the two beams pass through the same optical system, and the reference mirror is placed very close to the reflecting object. As a result, the effect of parasitic deformations and vibrations of the interferometer readout is reduced substantionaly.

We use a small shift of the beam splitter for rough adjustment of the beam before the measurements, and PZT-driven reference mirror for fine adjustment. The feedback loop is used for the interferometer locking. This loop consists of the detector, low pass filter, comparator and PZT-drive amplifier. The cut-off frequency of the filter is 1 Hz, therefore this loop allows to exclude the effect of slow variations of the arm length and the laser frequency.

The signal processing system includes low noise amplifier, band pass filter, ADC converter and PC386 computer running specially designed software. Additional rejection filter is used to decrease a 50 Hz power supply frequency to avoid a saturation of the amplifier. The noise factor of the amplifier is 3 dB, cuts of frequencies of the band pass filter are 0.5 and 1.5 kHz, the slope is 40 dB/oct.

The software allows i) to make records of the signal with the sampling rate from 2 to 40 kHz, ii) to realize digital filtering and spectrum analysis and iii) to store the information on hard disk. It is also possible to have a real time view of the

waveform or signal spectrum.

The experimental device includes 2 stages of the anti-seismic isolation. First is a passive filter consisting of four rubber springs on which the vacuum chamber is placed. The second stage is the rubber/brass multilayer support of the interferometer inside the vacuum chamber. These filters provide sufficient attenuation for the vibrations of the laboratory floor in the 1kHz frequency domain. However, the low frequency performance of the filters remains rather poor, and any artificial shocks at the laboratory may cause observable responses in the readout signal.

At the present time, the achieved sensitivity of the measurement system is $\simeq 4\times10^{-10}$ cm in the frequency band $\Delta f=0.5$ - 1 kHz.

The fragment of the record of noise oscillation of tungsten wire, stressed to $\eta=0.9\cdot\eta_B$ (where $\eta_B$ is the break stress) is shown in Fig.5. The mean amplitude is close to the predicted value of thermal fluctuations of the wire. Each point is a result of averaging over $10^{-1}$sec. Excess peaks of amplitude are observed in the record. The rate of peaks depends weakly on the time interval after applying of the stress and does not change considerably during several days of observations.

Number of amplitude peaks exceeding the level $k\sigma$ (where $\sigma$ is the variance of the absolute value of the coordinate) for two wires with stress $\eta_1\simeq0.5\cdot\eta_B$ and $\eta_2\simeq0.9\cdot\eta_B$ are presented in Table 1. The third column gives the number of peaks, corresponding to the normal distribution for the pure brownian motion. The data were collected during $1,2\cdot10^4$sec.

The results presented in Fig.5 and the Table 1 may be considered as arguments in favor of the existence of random jumps of local tension in stressed wire. The rate of the jumps substantially increases with the increasing stress. These results evidently translate into recommendation to design the suspension system with stresses much smaller than the value $\eta_B$.

We are planing to collect more data with wires fabricated of different materials and sizes in 1996, 1997 and to get a quantitative recommendation for a low excess noise suspensions.

## 3. Distortional mechanical effects in the wire suspension.

In addition to the program aimed at detection and analysis of the excess noise in the violin mode of the suspension an independent research was performed. The goals of this research were to detect and to record the basic macroscopic distortional effects in the wire suspension when the stress is close to the threshold of plastic deformation: i) to record residual deformation in the loaded wire, ii) to record the monotonous longitudinal drift, iii) to record the monotonous torsional drift, iv) to detect the relatively big angular jumps in the loaded wire.

To perform this task, an installation was built in which the key element was a torsional pendulum suspended on a tungsten wire with length L=10 cm and diameter $D=2\cdot10^{-3}$ cm. The wire was loaded by the weight of a variable mass. Measurements were done in the dynamical range of the stress from $\eta=0.2\cdot\eta_B$ to $\eta=0.9\cdot\eta_B$ (the breaking stress of thin tungsten wire is $\eta_B=4\cdot10^{10}$ dyn/cm$^2$, close

to $1 \cdot 10^{-2}$ of the Young modulus). The readout system consisted of two parts. The first one is a simple capacity sensor permitting to record elongation of the wire with the resolution $\Delta L/L \simeq 5 \cdot 10^{-5}$. The second one - an optical "lever" which permits to record the angular displacement of the pendulum with the resolution $\simeq 10^{-6}$ rad (Fig.6).

The main empirical results of these measurements are;

1) The effect of microplasticity (the residual deformation in the elongation of the wire after application of stress) which we recorded from the level of the stress $\eta = 0.4 \cdot \eta_B$ up to $\eta_B$. It is shown on the Fig.7.

II) We also observed that the residual deformation is accompanied with a monotonous drift of the length of the wire (the creep effect). Fig.8 illustrates this effect.

III) Monotonous drift of the wire's angle was also observed (see Fig.9). It is important to note that the rate of this drift does not decrease at low stresses ($\eta \lesssim 0.2 \cdot \eta_B$).

IV) The most important result of this set of measurements was the observation of relatively large jumps of the angle of torsion. The amplitude of these jumps was between $5 \cdot 10^{-5} - 3 \cdot 10^{-4}$ rad and large jumps appear under $\eta \gtrsim 0.7 \cdot \eta_B$ with the rate $\simeq 1$ jump per hour. When the value of $\eta$ approaches to $\eta_B$ the rate goes up.

In conclusion of this section let us estimate the displacement of interferometer mirror after such jump in one of two suspension wires assuming angle of torsion $\Delta\varphi \simeq 10^{-6}$. For simplicity we assume that this jump appears instantly at point of suspension and we are interested the displacement of mirror over

time $\Delta t=10^{-2}$ s after this event.

Instantaneousness means that jump happens during time much shorter than $\Delta t$. The time after which the lower end of wire starts "to feel" this shift is also $\ll \Delta t$. Under these assumptions we can consider the problem as constant twisting of wire that corresponds to constant torque $M=(\pi/2)\ G\ r^4 L^{-1}\ \Delta\varphi \simeq 3.5\cdot10^{-5}$ dyn·cm (here $G=1.5\cdot10^{12}$ dyn/cm$^2$ - is the shear modulus, $r=5\cdot10^{-3}$cm - is the radius of wire and L=40 cm - is length of wire), applied to mirror.

The time $\Delta t$ is also much shorter than period of torsional oscillations of the mirror (on two wires). Therefore the mirror can be considered as a free mass and therefore we obtain that during time $\Delta t$ it should turn by angle $\vartheta$ relatively to its center of mass:

$$\vartheta=M\Delta t^2/(2J) \simeq 6\cdot10^{-14},$$

where $J=m(R^2/4+H^2/12)$ - is the moment of inertia, m - is the mirror mass, R and H - are its radius and height. In above estimates we put m=2 kg, R=5cm, H=10 cm.

It should be underlined that the center of mass of mirror does not move. However, if the middle of interferometer probe beam crossection is displaced by value $\Delta r \simeq 5\cdot10^{-3}$cm with respect to its center, then the effective distance between interferometer mirrors is changed by value $\Delta x = \Delta r\cdot\vartheta \simeq 3\cdot10^{-16}$cm. It should be noted that this value is larger than the prediction of gravitational wave signal.

## 4.The fluctuations and changes of the magnetic field in the laboratory.

The use of D.C. magnet in the actuator (which provides the force acting on the mirror) may create a force which mimics the bursts of gravitational waves due to relatively rare random changes and fluctuations of the magnetic field in the laboratory. The A.C. components of the magnetic field in the ranges 50-150 Hz, their random changes and the level of magnetic noise between the harmonics (50 Hz, 100 Hz, 150 Hz) were measured. We used a coil (250 turns and 600 $cm^2$ square area) which had a transfer factor 0.4 V/Gauss at the industrial power supply frequency 50Hz. Using this coil, an amplifier and oscillograf we find that in the ordinary lab the pick-to-pick amplitude of the magnetic field may be from $3 \cdot 10^{-2}$ Gauss up to $1 \cdot 10^{-4}$ Gauss depending on the location of the coil between the pieces of electronic equipment. The characteristic length along which this amplitude of the magnetic field changes with the factor 2 is 50 cm - 100 cm. The spectral component of the recorded signals consists of the harmonics of the industrial frequency and considerable noise between them. The peak-to-peak amplitude is not stable and it changes substantially if nearly electrical devices are switched "on" or "off". For example if rectifier (400 Watt power) is switched "on" or "off" at the distance $3 \cdot 10^2$cm from the coil it produces the jumps of amplitude at the level $(1-2) \cdot 10^{-3}$gauss with the duration of the front $\simeq 10^{-2}$sec. At the same distance another piece of electronics (100 Watt source of standard signals) produces jumps with the amplitude $3 \cdot 10^{-4}$ gauss.

The results of the preliminary measurements of the level of the magnetic noise between the harmonics may be described as follows

| The frequency range | |
|---|---|
| 60 - 70 Hz | $1 \cdot 10^{-6}$ gauss $Hz^{-1/2}$ |
| 80 - 90 Hz | $4 \cdot 10^{-7}$ gauss $Hz^{-1/2}$ |
| 110 - 120 Hz | $2 \cdot 10^{-7}$ gauss $Hz^{-1/2}$ |

The obtained preliminary results of the measurements of jumps of the magnetic field in MSU (being extrapolated into the lab at Caltech) directly indicate that these jumps may mimic the gravitational wave bursts orders larger than the expected amplitude of the perturbation of the metric. Simple calculations also show that the measured values of the magnetic noise "floor" may make a substantial contribution into the noise floor of currently working prototype.

## CONCLUSION

1) The experimental measurement of quality factor of low frequency modes of the test mass prototype, with the intermediate mass value M ≈ 2 kg, suspended on fused silica fibers, have shown that the pendulum modes have $Q_{pend} \approx (0.5 - 1) \cdot 10^8$, similar to that in low mass (M = 30g) prototypes. The obtained values of $Q_{pend}$ and $Q_{violin}$ allow to reach the standard quantum limit of the sensitivity if averaging time $\tau \leqslant 10^{-3}$s.

2)The first study of noise oscillations in the stressed thin wires, which model the behavior of the test mass suspension, have shown that the rare jumps of amplitude with the value of several standard deviations are added to the Brownian motion of the wire. This jumps are caused by internal processes in the wires. They can mimic the output signal of the antennae and require detailed investigation.

3)The results of measurement of the laboratory magnetic field (including fast jumps) indicate, on our opinion, that the use of the dc magnets in actuator may be a serious obstacle for reaching the planned sensitivity of the antennae.

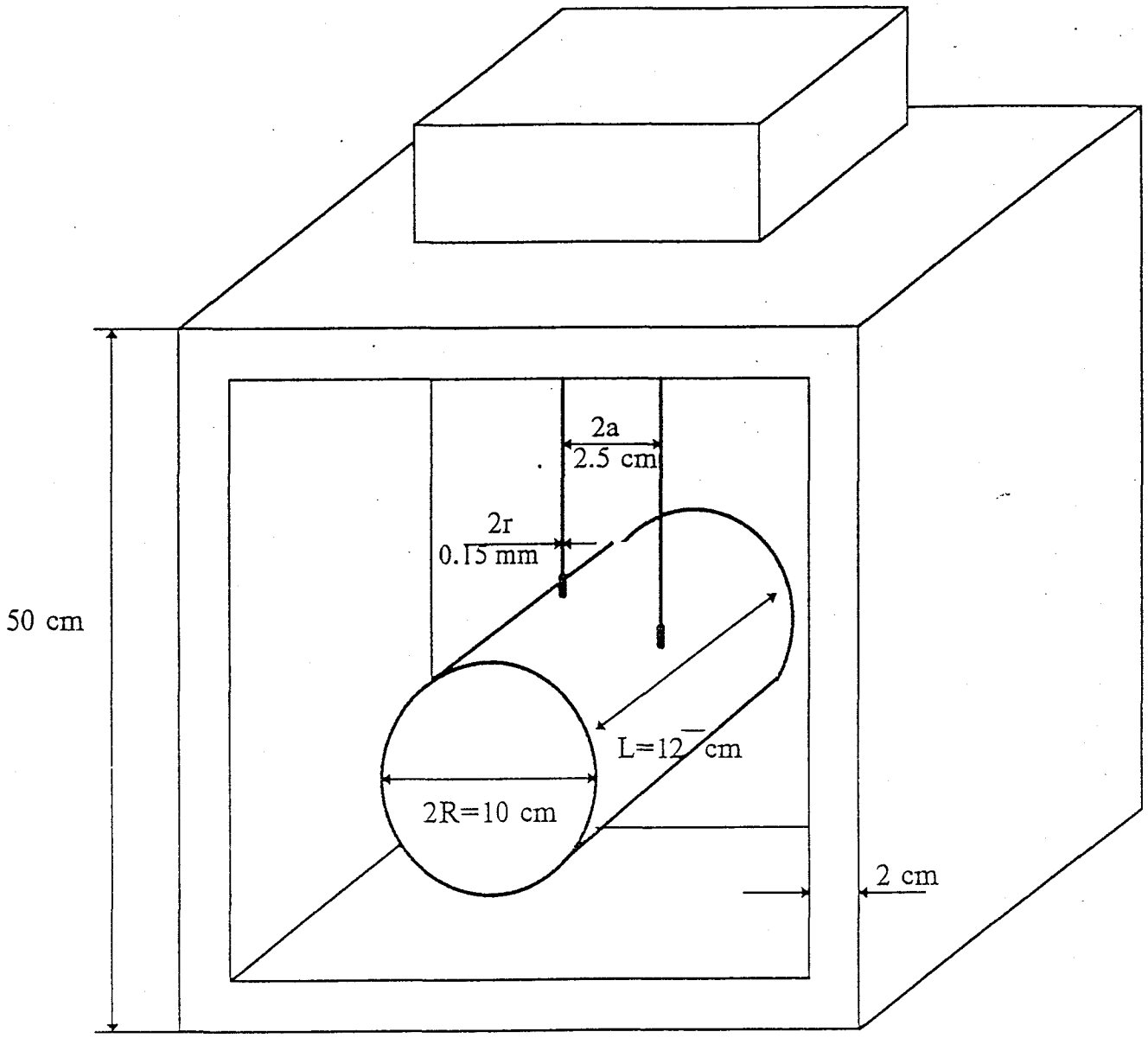


Fig. 1. Design of the double fiber pendulum and its support.

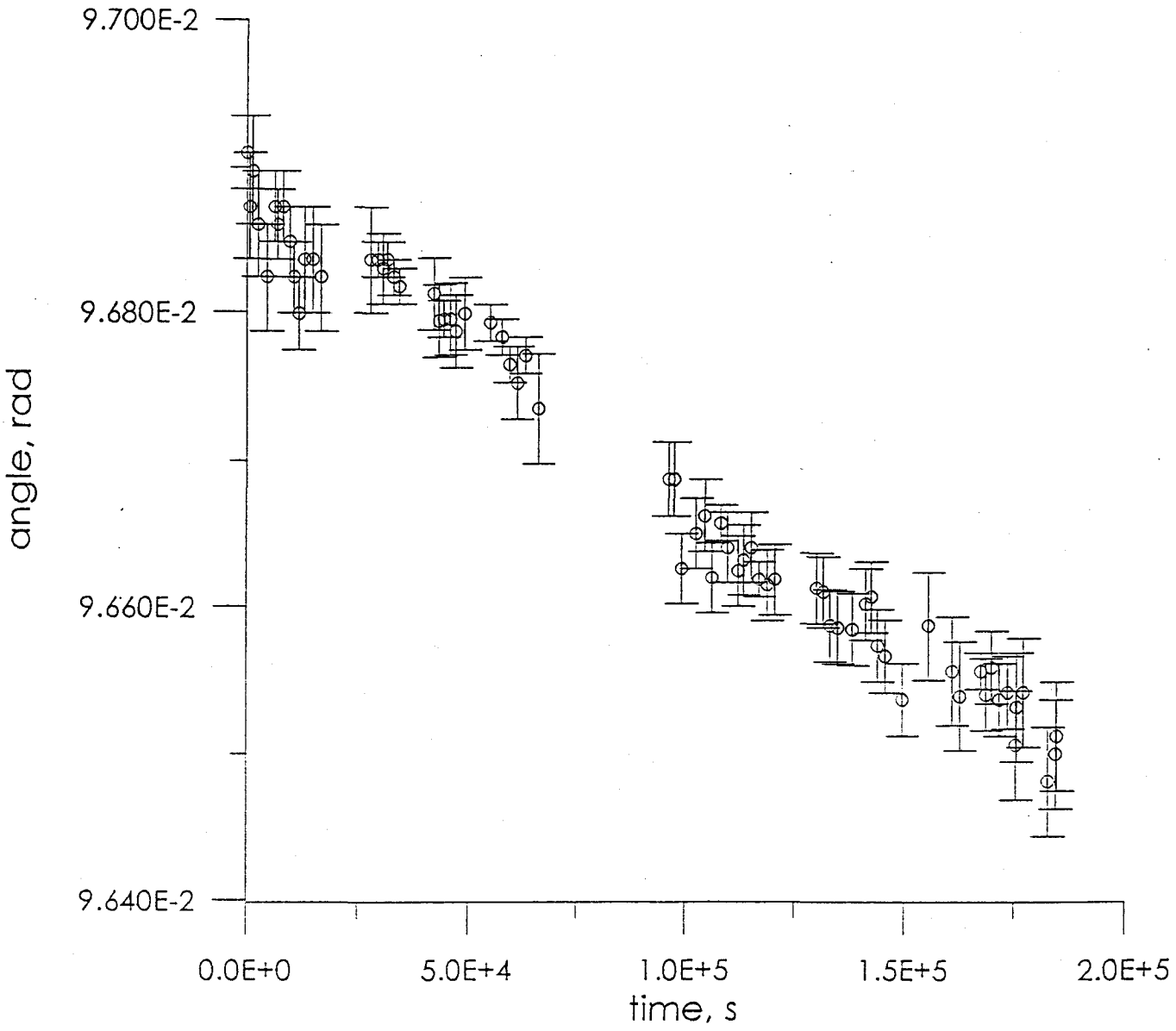


Fig. 2 . Time dependence of amplitude of the double fiber pendulum № 1
(M = 2 kg., $d_{fiber}$ = 150-200 mkm, T=2.85 s).
The measured time of relaxation $\tau^* = 4.8*10^7$ s (±2 %).
With extraction of residual gas damping ( p = $2*10^{-6}$ Torr)
$\tau^* = 1*10^8$s. (±25%)

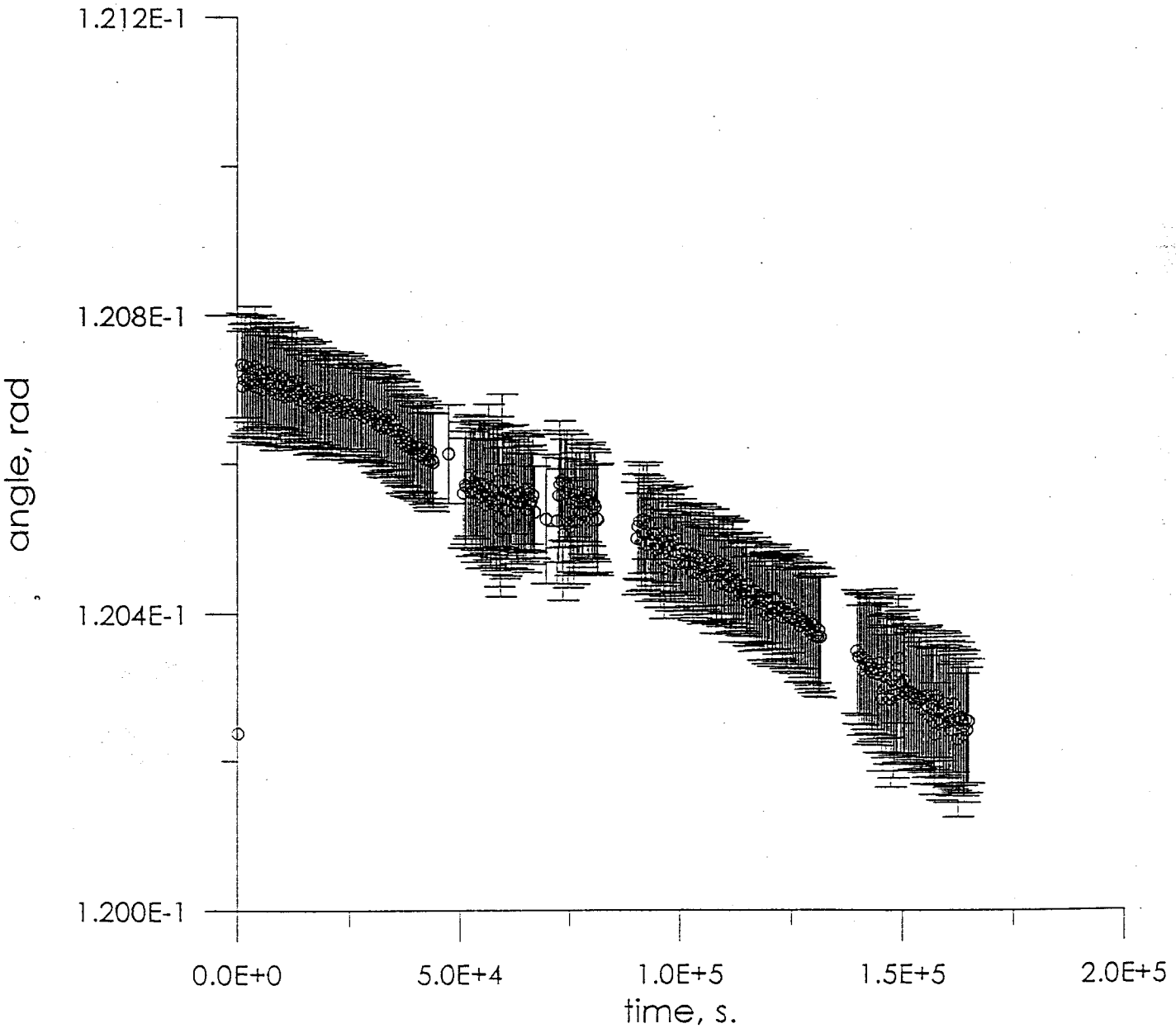


Fig. 3 . Time dependence of amplitude of the double fiber pendulum № 2
(M = 2 kg., $d_{fiber}$ = 150-200 mkm, T=2.95 s).
The measured time of relaxation $\tau^* = 4.6*10^7$ s (±2 %).
With extraction of residual gas damping ( p = $1*10^{-6}$ Torr)
$\tau^* = 6.5*10^7$ s. (±25%)

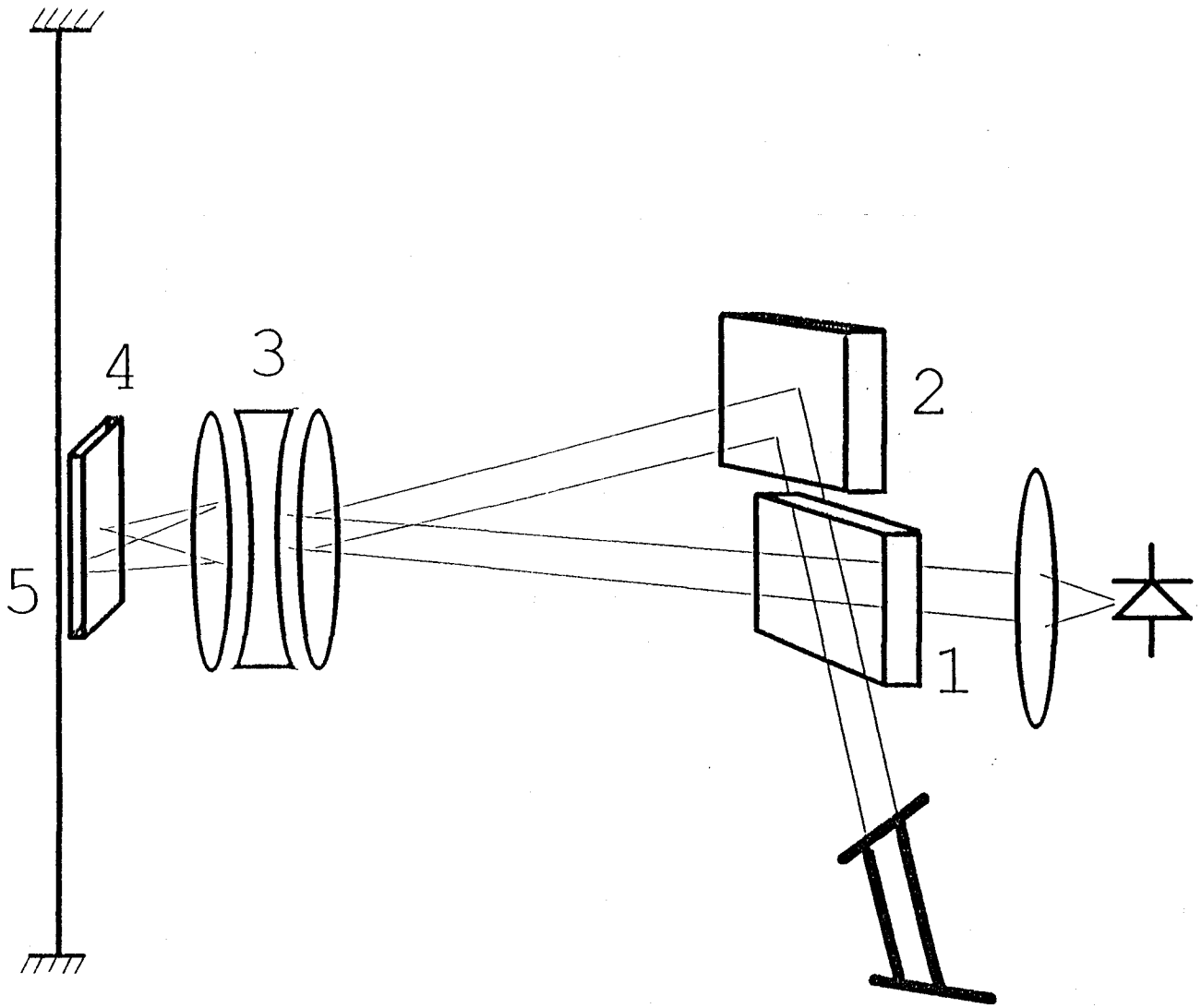


Fig. 4. Experimental setup for excess noise measurement in suspension wires.

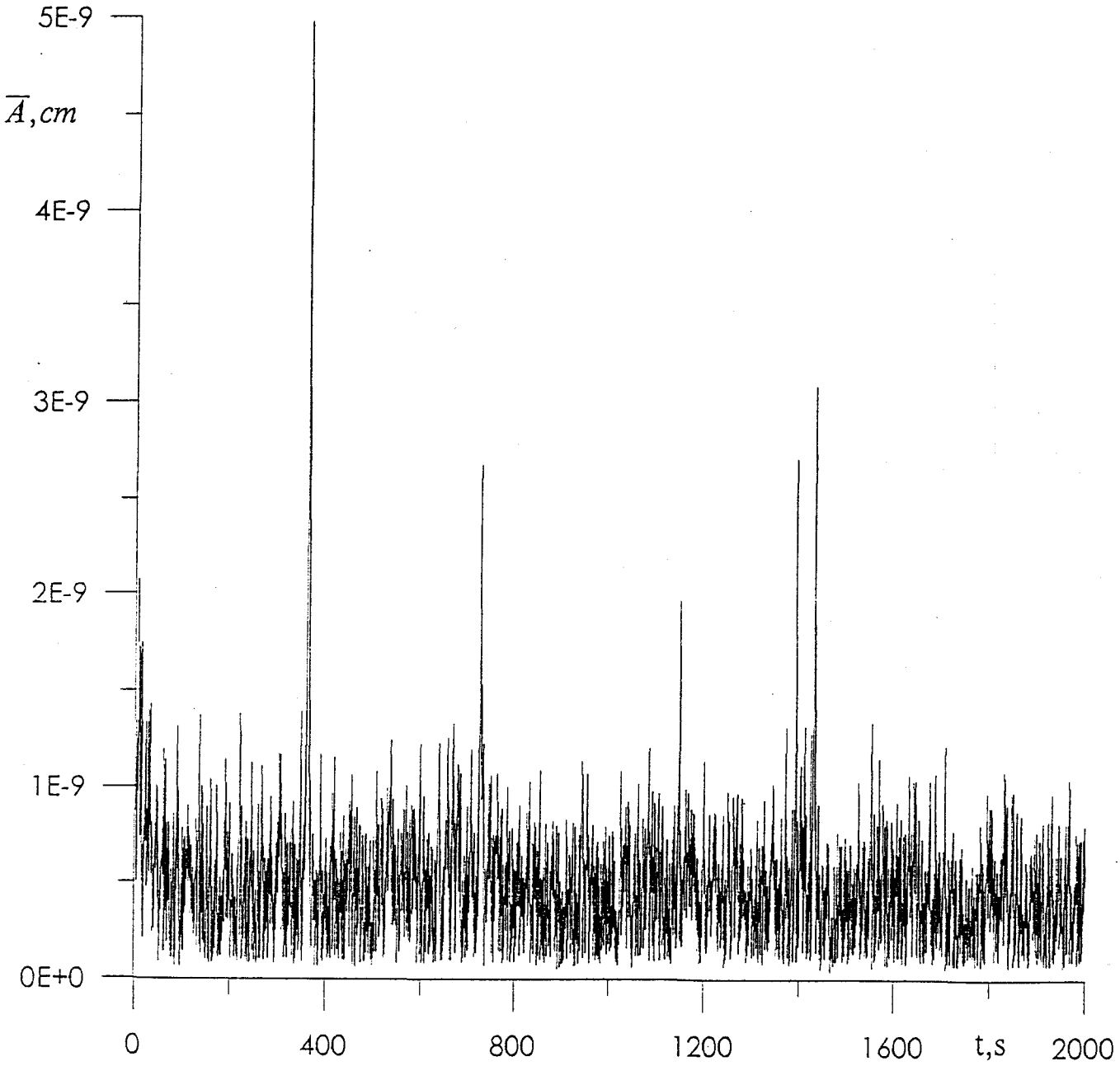


Fig. 5. Fragment of the record of noise oscillation of tungsten wire

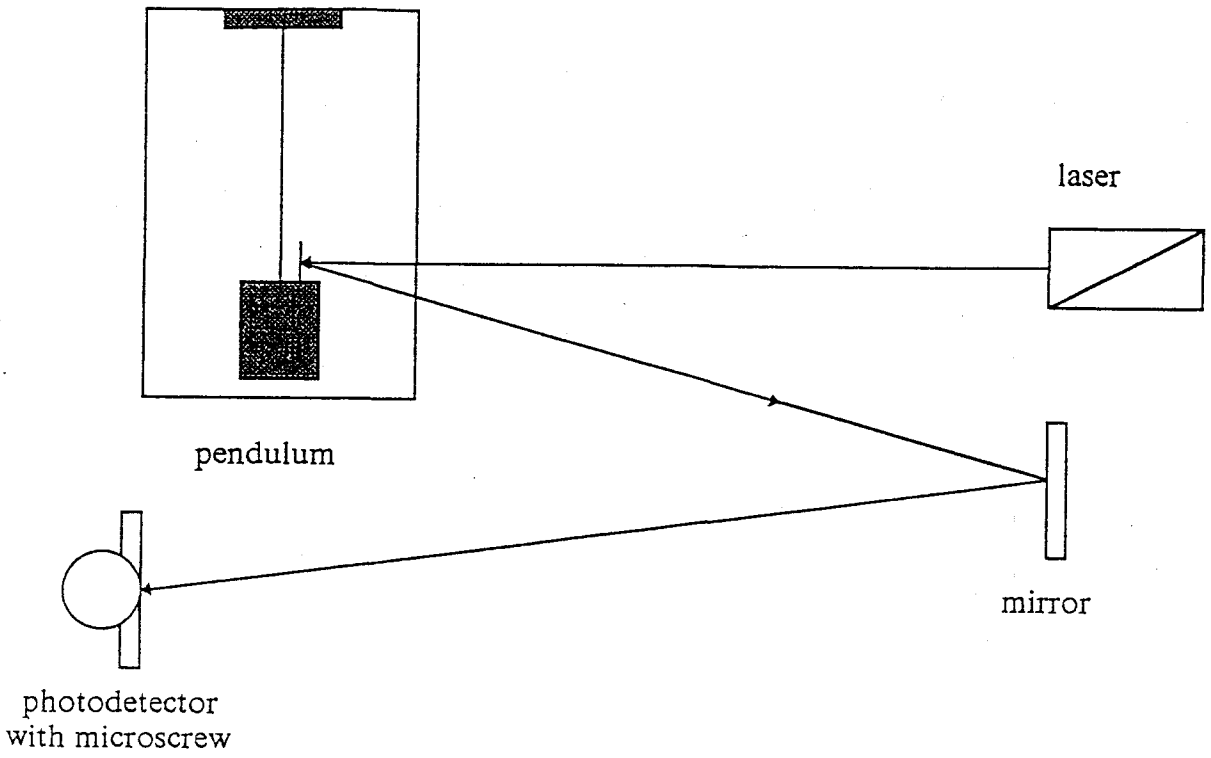


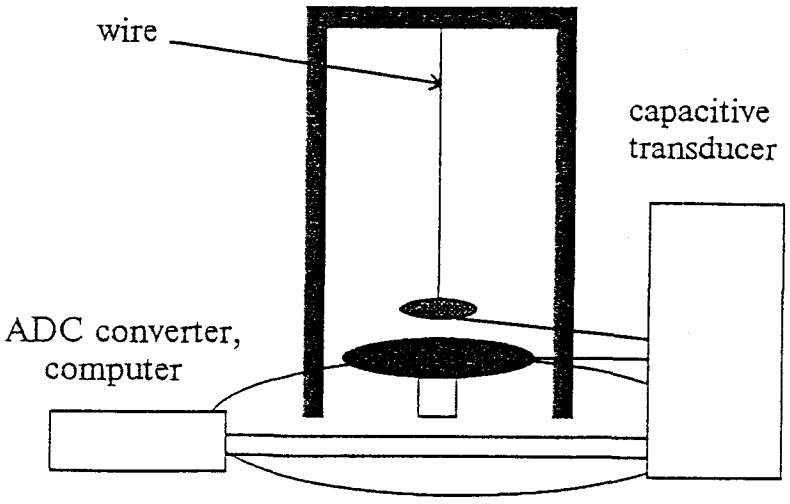


Fig. 6. Experimental setup for measurments of angular displacement and elongation of the wire.

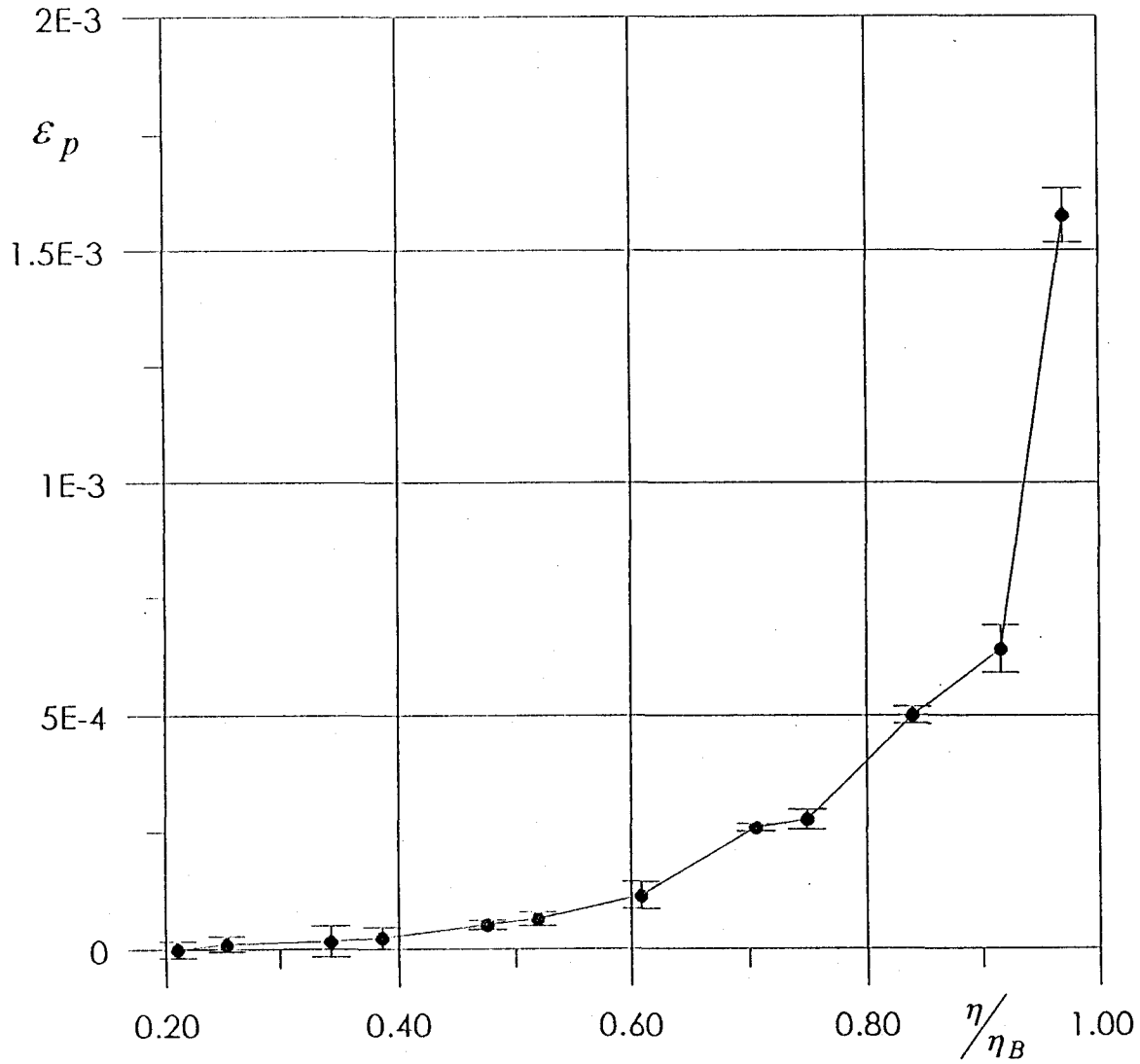


Fig.7 . Microplasticity of tungsten wire.

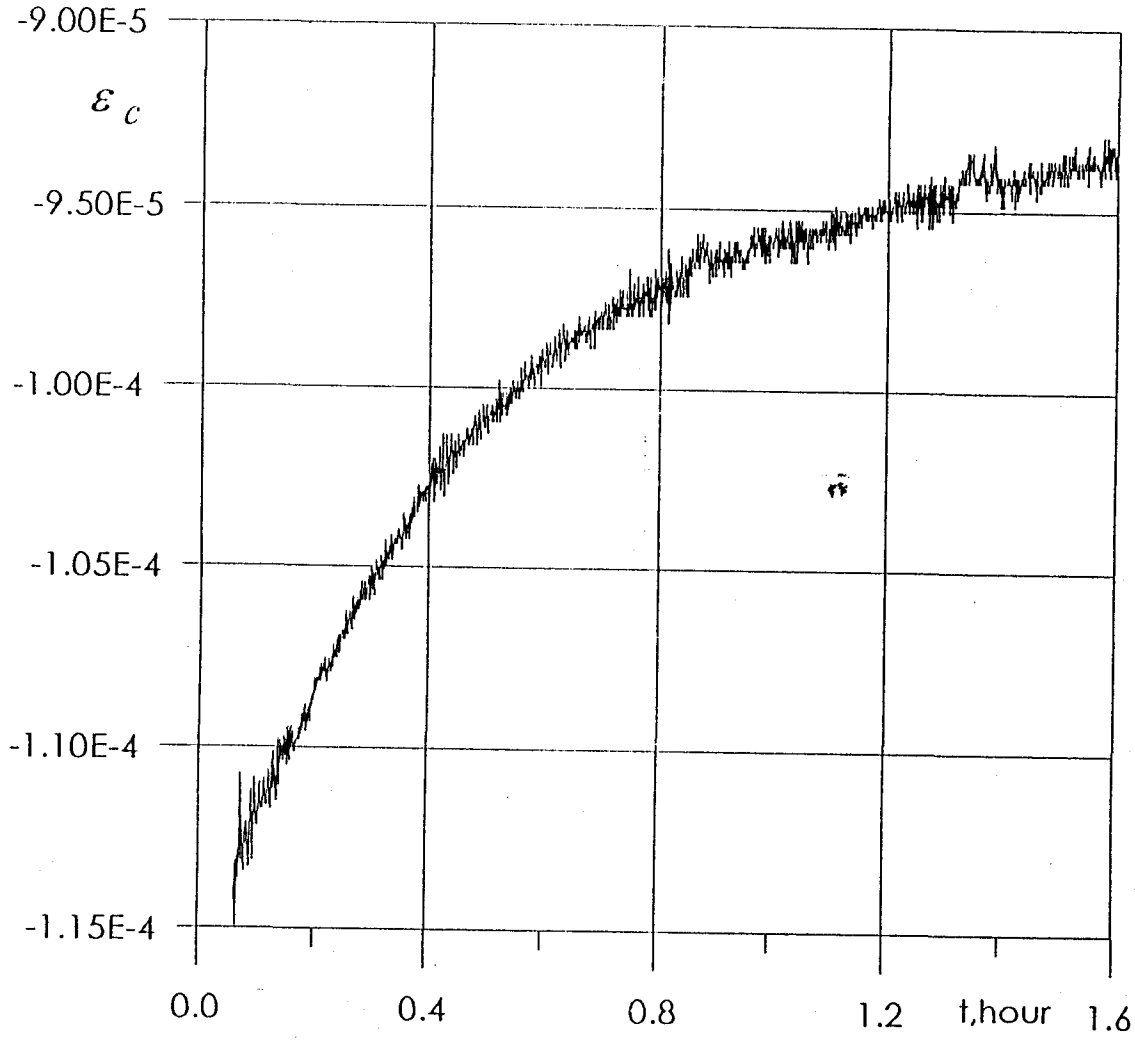


Fig. 8. Creep of tungsten wire (stress $\eta = 0.35\eta_B$).

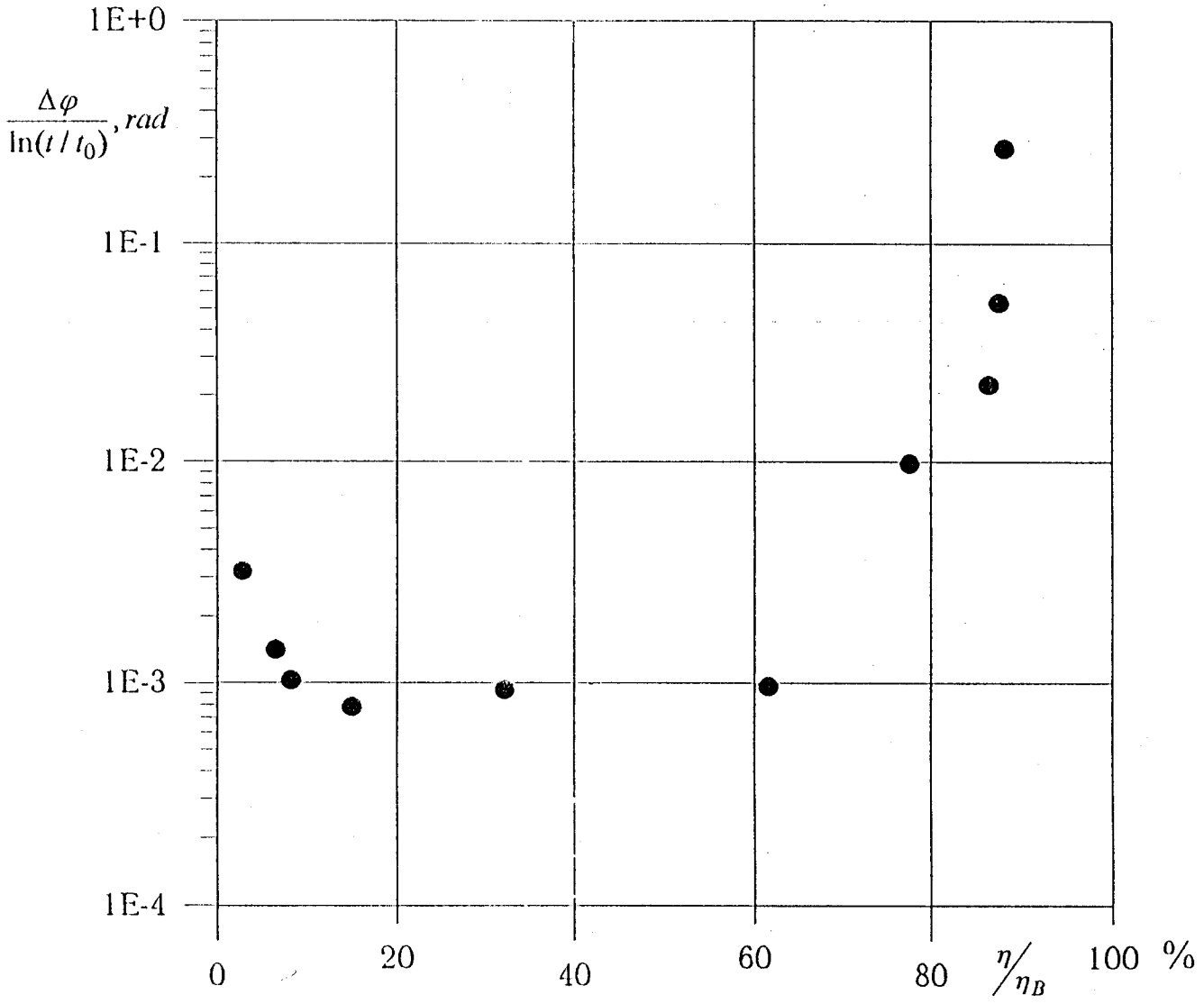


Fig. 9. Stress dependence of the angular drift rate of the wire.

TABLE 1

Number of amplitude peaks exceeded the given level

| | Low stressed sample $\eta=0.5\eta_B$ | Well stressed sample $\eta=0.9\eta_B$ | Theory |
|---|---|---|---|
| >10 σ | 0 | 298 | <<1 |
| > 9 σ | 0 | 341 | <<1 |
| > 8 σ | 4 | 427 | 0.19 |
| > 7 σ | 11 | 563 | 3.2 |
| > 6 σ | 38 | 800 | 38 |
| > 5 σ | 270 | 1478 | 320 |
| > 4 σ | 1748 | 3848 | 1900 |